Journal of Alloys and Compounds 512 (2012) 355–360

Contents lists available at SciVerse ScienceDirect

Journal of Alloys and Compounds

journal homepage: www.elsevier.com/locate/jallcom

Effect of hot extrusion on microstructures and mechanical properties of SiC nanoparticles reinforced magnesium matrix composite

K.B. Nie[a], X.J. Wang[a,b,*], L. Xu[a], K. Wu[a,b], X.S. Hu[a], M.Y. Zheng[a]

[a] School of Materials Science and Engineering, Harbin Institute of Technology, No. 92. West Da-Zhi Street, Harbin 150001, PR China
[b] National Defense Science and Technology Key Lab for Space Materials Behavior and Evaluation, Harbin Institute of Technology, No. 92. West Da-Zhi Street, Harbin 150001, PR China

ARTICLE INFO

Article history:
Received 23 August 2011
Received in revised form
30 September 2011
Accepted 30 September 2011
Available online 8 October 2011

Keywords:
Magnesium matrix nanocomposite
Dynamic recrystallization
Extrusion
Grain size
Tensile properties

ABSTRACT

Particulate reinforced magnesium matrix nanocomposite prepared with semisolid stirring assisted ultrasonic vibration was subjected to extrusion at 350 °C with an extrusion ratio of 12:1. Extrusion of the SiCp/AZ91 nanocomposite induced large scale dynamic recrystallization resulting in a fine matrix microstructure. There were two kinds of zones in the extruded nanocomposite: SiC nanoparticle bands parallel to the extrusion direction and refined-grain zones between the SiC nanoparticle bands. In the SiC nanoparticle bands, there were SiC nanoparticles along the boundaries of refined grains. The distribution of SiC nanoparticles was uniform although some agglomerates of SiC nanoparticles still existed in the SiC nanoparticle bands. The ultimate tensile strength, yield strength and elongation to fracture of the SiCp/AZ91 nanocomposite were simultaneously improved by extrusion. Results from the extruded SiCp/AZ91 nanocomposite tensile testing at different temperatures (75, 125, 175 and 225 °C) revealed an increase of the tensile strength and ductility values compared with the unreinforced and extruded AZ91 alloy.

1. Introduction

In order to improve the mechanical properties of Mg, significant efforts have been taken to develop magnesium matrix composites (MMCs) due to their low density and superior specific properties including strength, stiffness and creep resistance [1–8]. Compared with the unreinforced magnesium alloys, tensile strength and elastic modulus of the micro particles reinforced MMCs are normally improved, but their ductility is reduced, which limits their widespread application. The desired properties can be achieved by a judicious selection of the type of reinforcing particles. Thus, use of nanoparticles to reinforce metallic materials (including Mg) has inspired considerable research interest in recent years because of the potential development of novel composites with unique mechanical and physical properties [9,10].

Processing technique is the key to fabrication of magnesium matrix nanocomposites with optimized properties. In general, metal matrix nanocomposites are widely made with expensive powder metallurgy, ball milling, deposition, infiltration techniques and ultrasonic vibration [11–19]. Recently, a novel technique that combined stir casting with ultrasonic vibration has been used to achieve a uniform dispersion and distribution of nanoparticles in magnesium melts [20]. It is considered that semisolid stirring can be utilized to incorporate the nanoparticles and disperse them macroscopically while the strong impact coupled with local high temperatures introduced by ultrasonic vibration can break nanoparticle clusters and clean their surface from the view of microcosmic [20,21]. These investigations on magnesium matrix nanocomposites confirm that nanoparticles have a positive influence on mechanical properties of Mg.

To further extend the applications of magnesium matrix nanocomposites in the automotive and other weight critical industries, an improvement in the mechanical properties and ductility is required. At present, considerable interest is devoted to study the effect of secondary processing on metal matrix composite reinforced with micro ceramic particles. Several plastic deformation processes, such as extrusion, rolling and forging, have been successfully used to enhance the strength and ductility of micro particles reinforced composites [22–24]. Among these techniques, extrusion is very useful for its technical and economic advantages in the production of structural components, which yields a full integrity wrought material [25].

In fact, no research on the extrusion of nanoparticles reinforced AZ91 magnesium matrix nanocomposites, especially, when fabricated by semisolid stirring assisted ultrasonic vibration, has been reported in the open literature. Therefore, the aim of the present work is to investigate the influence of hot extrusion on the microstructures and mechanical properties of a particulate reinforced magnesium matrix nanocomposite.

* Corresponding author. Tel.: +86 45186402291; fax: +86 45186413922.
E-mail addresses: kaibo.nie@gmail.com (K.B. Nie), xjwang@hit.edu.cn (X.J. Wang).

0925-8388/$ – see front matter © 2011 Elsevier B.V. All rights reserved.
doi:10.1016/j.jallcom.2011.09.099

2. Experimental procedures

2.1. Materials

A commercial AZ91 alloy (supplied by Northeast Light Alloy Company Limited, China) with a nominal composition of Mg–9.07Al–0.68Zn–0.21Mn was employed as the matrix. SiC nanoparticles (supplied by Hefei Kaier Nanometer Energy & Technology Company Limited, China) with an average size of 60 nm and volume fractions (vol.%) of 1% were selected as the reinforcement. The SiCp/AZ91 nanocomposites were fabricated by semisolid stirring assisted ultrasonic vibration and then homogenized at 415 °C for 24 h (T4 treatment). The details of fabrication process were described in Ref. [20].

2.2. Extrusion of materials

The extrusion was conducted using a press with a 2000 kN load limit. Billets after T4 treatment were approximately 60 mm in diameter by 70 mm. The billets, pressure pad and dish-shaped die were put into the extrusion container. The extrusion container was heated to 350 °C in a muffle furnace. The temperature of the container was monitored using a K-type thermocouple inserted into a hole drilled in the container. Once the container attained the desired temperature, a period of 1 h was allowed to elapse before the extrusion was carried out. This time is long enough to allow the billet to reach a steady-state temperature, as determined from previous tests. The billets were extruded with an extrusion ratio of 12:1 and constant RAM speed of 15 mm s^{-1} and then cooled in air. For the purpose of comparison, an AZ91 alloy ingot without semisolid stirring assisted ultrasonic vibration was also cast and extruded under the same conditions.

2.3. Microstructural characterization

Optical microscopy (OM), scanning electron microscopy (SEM) and transmission electron microscopy (TEM) were used to study the evolution of the matrix and the nanoparticle distribution introduced by extrusion. Samples for microstructure analysis were carried out in the central part of specimens parallel to the extrusion direction and prepared by the conventional mechanical polishing and etching using acetic picral [5 ml acetic acid + 6 g picric acid + 10 ml H_2O + 100 ml ethanol (95%)]. In order to measure the grain size of the nanocomposites before and after extrusion, Image-Pro Plus (IPP) software was used to determine the linear intercept length of at least 2000 grains of matrix in the nanocomposites. Microstructural features of the SiCp/AZ91 nanocomposite were identified using energy dispersive spectrophotometric (EDS) analysis. Specimens for TEM were prepared by grinding-polishing the sample to produce a foil of 50 μm thickness followed by punching 3 mm diameter disks. The disks were ion beam thinned.

2.4. Tensile test

To determine the tensile properties, the samples were machined parallel to the extrusion direction. The tensile tests were carried out by Instron-1186 tension machine at 25, 75, 125, 175 and 225 °C and the tensile rate was 0.5 mm/min. The furnace and tensile grips were preheated to the test temperature. The test specimens were then loaded into the tensile grips and the furnace was re-heated to testing temperature. The specimens were held at the testing temperature for 10 min before testing to ensure a uniform temperature distribution.

3. Results and discussion

3.1. Microstructure evolution during extrusion

Fig. 1 illustrates OM micrographs of the SiCp/AZ91 nanocomposites before and after extrusion. It can be observed from Fig. 1 that grains of matrix in the SiCp/AZ91 nanocomposite are significantly refined after extrusion. Fig. 2 shows distribution of grain size for the SiCp/AZ91 nanocomposites before and after extrusion. In the as-cast nanocomposite, some SiC nanoparticles are distributed along the grain boundaries and the average grain size of matrix is about 84 μm, as shown in Figs. 1(a) and 2(a). This can be attributed to the "push effect" of the solidification front during the growth of primary magnesium grains resulting from the manufacturing technique [20]. There are two kinds of zones in the extruded nanocomposite: SiC nanoparticle bands parallel to the extrusion direction and refined-grain zones between the SiC nanoparticle bands, as shown in Fig. 1(b). The average grain size of the extruded SiCp/AZ91 nanocomposite is about 6 μm, which indicates that full dynamic recrystallization (DRX) occurs during extrusion. DRX is thought to initiate at original grain boundaries (prior to extrusion) due to an accumulation of dislocations at the grain boundaries during the hot extrusion [26]. The grain size of the extruded nanocomposite is also

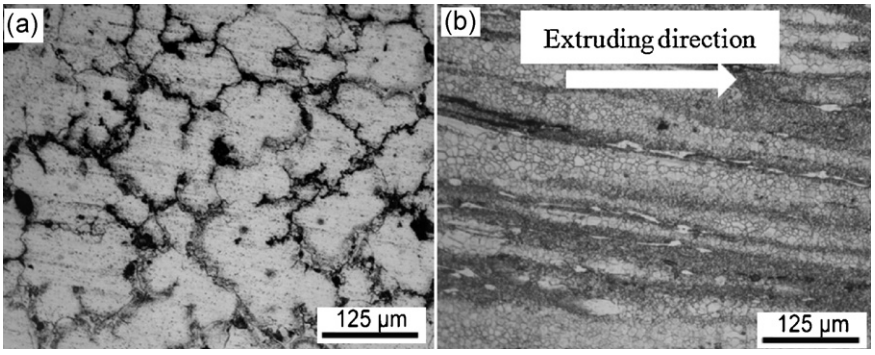

Fig. 1. OM micrographs of the SiCp/AZ91 nanocomposite: (a) as-cast and (b) as-extruded.

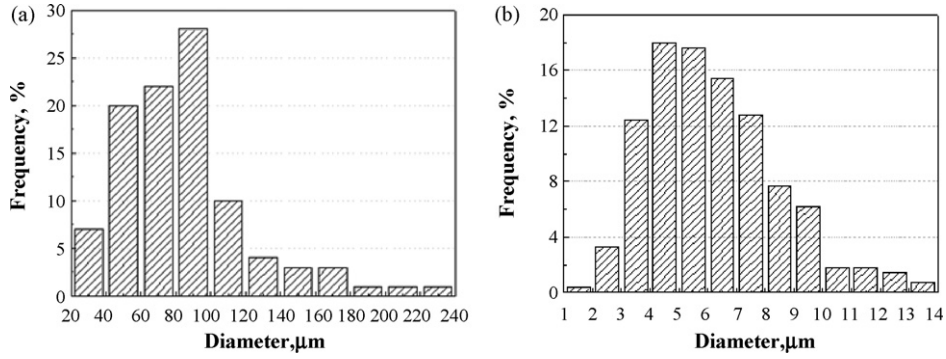

Fig. 2. Distribution of grain size for the SiCp/AZ91 nanocomposite: (a) as-cast and (b) as-extruded.

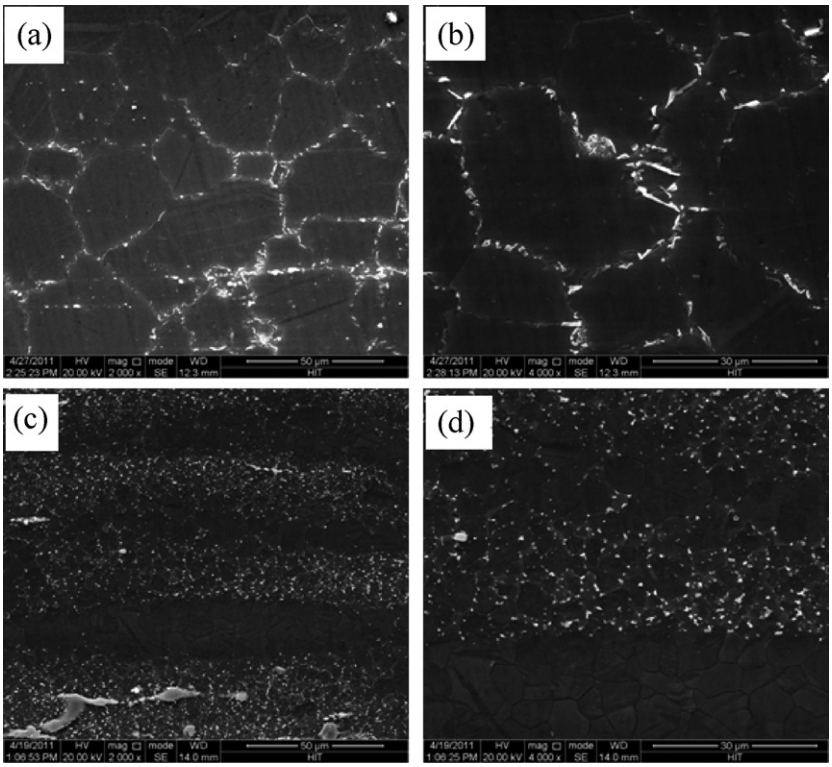

Fig. 3. SEM micrographs of (a) as-extruded AZ91 alloy and (c) as-extruded SiCp/AZ91 nanocomposite; higher magnification of (b) as-extruded AZ91 alloy and (d) as-extruded SiCp/AZ91 nanocomposite.

inhomogeneous with small grains of about 2–4 μm and large grains of 14 μm as shown in Fig. 2(b). The grains in the SiC nanoparticle bands are finer than that in the refined-grain zones (in Fig. 1b), which indicates that DRX in the SiCp/AZ91 nanocomposite is sensitive to the nanoparticle content on a local scale. On the one hand, the severer DRX could occur with the larger strain due to the addition of SiC nanoparticles in the particle bands. On the other hand, the addition of SiC nanoparticles may lead to a significant inhibition in grain boundaries migration of SiCp/AZ91 nanocomposite resulting in the refined grains after extrusion.

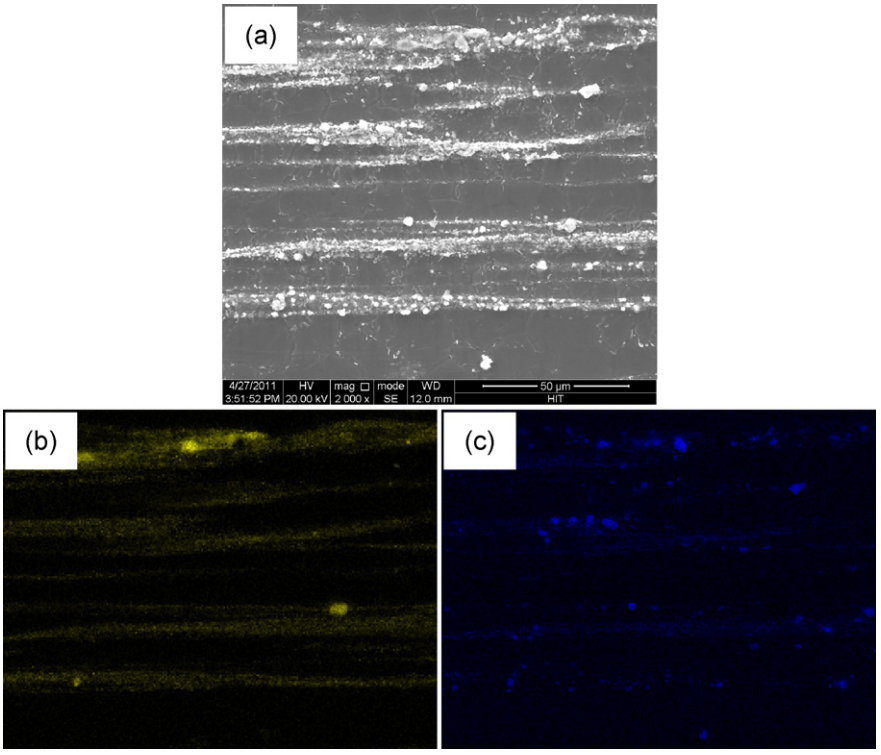

Fig. 4. SEM micrographs of (a) as-extruded SiCp/AZ91 nanocomposite; EDS of (b) Si K and (c) Al K.

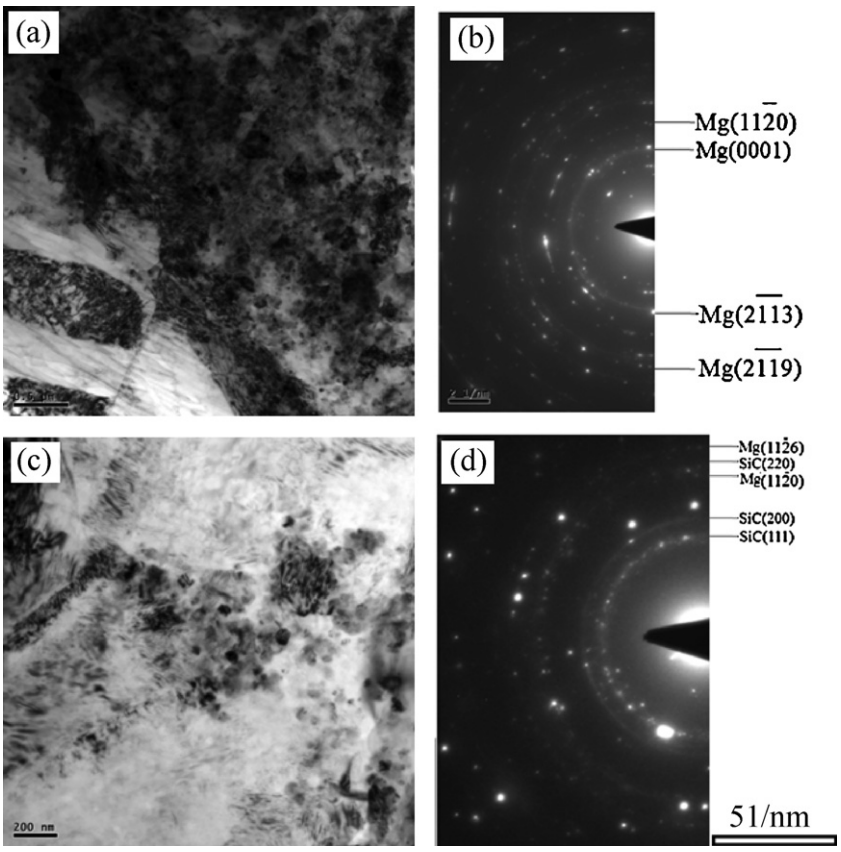

Fig. 5. TEM micrographs of SiCp/AZ91 nanocomposite after extrusion: (a) near the extrusion band; (b) electron diffraction near the extrusion band; (c) SiC nanoparticles; (d) electron diffraction of SiC nanoparticles.

As shown in Fig. 3, it can be found that grain size of matrix in the extruded SiCp/AZ91 nanocomposite is smaller than that of the extruded AZ91 alloy. This can be also attributed to the addition of SiC nanoparticles which can introduce the larger strain resulting in the severer DRX and inhibit grain growth effectively during the extrusion process. For the extruded AZ91 alloy (Fig. 3a and b), coarse grains with refined precipitated phase along the grain boundaries are observed. For the SiCp/AZ91 nanocomposite (Fig. 3c), SiC nanoparticle bands as well as refined-grain zones are observed, which is consistent with that as shown in Fig. 1(b). At higher magnification, the presence of small grains with SiC nanoparticles along the grain boundaries can be found in the SiC nanoparticle bands as shown in Fig. 3(d). This is similar to the DRX in the magnesium matrix composite reinforced with micro ceramic particles. Wang et al. [27] have found that there is more stored energy and larger driving force for nucleation in the particle-rich zones and at particle clusters in the micro particles reinforced magnesium matrix composite. So, it is expected and observed that recrystallized grains are finer in the SiC nanoparticle bands and between closed packed nanoparticles in the present nanocomposite.

EDS is used to investigate the composition of the bands observed in OM and SEM, as shown in Fig. 4. Analyzing an area of SEM micrograph in Fig. 4(a), EDS of Si K and Al K (Fig. 4b and c) demonstrate that composition of particle clusters in the SiC nanoparticle band is SiC nanoparticles. The distribution of EDS of Si K is homogeneous outside the SiC nanoparticle bands, which indicates that the distribution of SiC nanoparticle is uniform outside the SiC nanoparticle bands as shown in Fig. 4(a).

Fig. 5 shows TEM micrographs of the SiCp/AZ91 nanocomposite after extrusion. Some SiC nanoparticles are found to be agglomerated within the SiC nanoparticle band as shown in Fig. 5(a). This is in agreement with the nanoparticle cluster as shown in Figs. 3(c) and 4(a). In Fig. 5(d) the study of electron diffraction (ED) confirms that composition of the particle is SiC nanoparticles. At higher magnification, most of the SiC nanoparticles inside the cluster are still segregated by magnesium matrix as shown in Fig. 5(c). This indicates that distribution of the SiC nanoparticles can be further improved by hot extrusion. It can be also found that some fine grains with an average size of 20 nm exist near the SiC nanoparticle band as shown in Fig. 5(a) and confirmed by ED in Fig. 5(b), which is much smaller than the grain size obtained using OM. This can further confirm that the addition of SiC nanoparticles could effectively refine the grains.

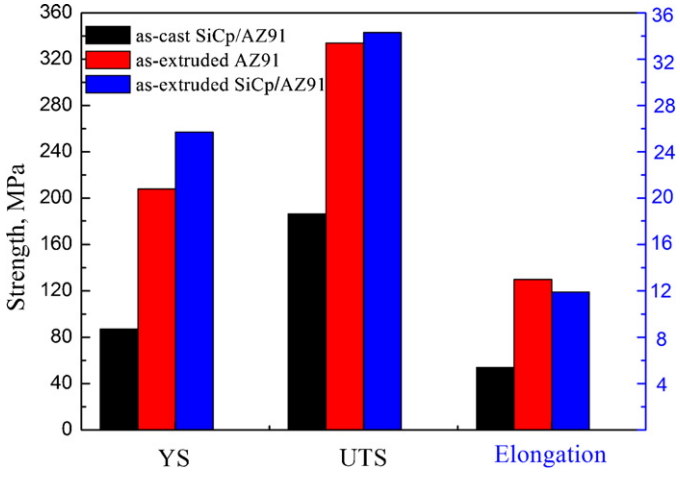

Fig. 6. Tensile strength of as-extruded AZ91 and SiCp/AZ91 nanocomposite at room temperature.

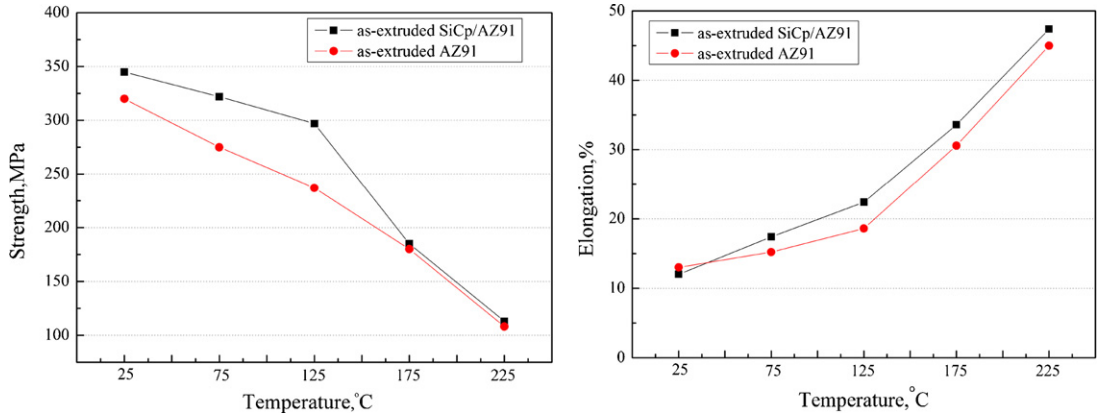

Fig. 7. Tensile strength of as-extruded AZ91 and SiCp/AZ91 nanocomposite at 25, 75, 125, 175 and 225 °C.

3.2. Evolution of the tensile properties during extrusion

Fig. 6 shows yield strength (σ_{YS}, 0.2% proof stress), ultimate tensile strength (σ_{UTS}, the ultimate tensile strength) and elongation to fracture of AZ91 alloy and SiCp/AZ91 nanocomposites before and after extrusion. Compared with as-cast nanocomposite, the extruded nanocomposite exhibits a simultaneous increase in yield strength, ultimate tensile strength and elongation to fracture. It can be also found that with the addition of SiC nanoparticles, the yield strength and ultimate tensile strength of the extruded SiCp/AZ91 nanocomposite are enhanced while elongation to fracture is slightly decreased compared with the extruded AZ91 alloy. According to the classic Hall–Petch equation: $\sigma_y = \sigma_0 + K_y d^{-1/2}$, where σ_y is the yield strength, σ_0 and K_y are material constants, and d is the mean grain size. The value of K_y is dependent on the number of slip systems. It is higher for HCP metals than for FCC and BCC metals [28]. The grains of matrix in the SiCp/AZ91 nanocomposite are refined after extrusion as shown in Fig. 1, as a result the yield strength of SiCp/AZ91 nanocomposite increases. The improvement of nanoparticle distribution in the nanocomposites after extrusion, as shown in Fig. 4, also contributes to the increase of ultimate tensile strength and elongation to fracture. In addition, grain size of matrix in the SiCp/AZ91 nanocomposite is smaller than that of AZ91 alloy with the same extrusion process (Fig. 3) resulting in higher yield strength. However, some agglomerates of SiC nanoparticles are still found in the extruded SiCp/AZ91 nanocomposite, which impairs the elongation to fracture.

The tensile strength and ductility conducted at various temperatures for the AZ91 alloy and SiCp/AZ91 nanocomposite after extrusion are shown in Fig. 7. It can be seen from Fig. 7 that tensile strength of SiCp/AZ91 nanocomposite is enhanced compared with the AZ91 alloy under all the test temperatures while the ductility is improved with the temperature range from 75 to 225 °C. Below recrystallization temperature for Mg and at 125°C there are moderate enhancements in tensile strength. The consistent increase in ductility with the addition of SiC nanoparticles with the temperature range from 75 to 225 °C is similar to the ductility increase that was previously reported with the addition of nanoparticles to pure Mg matrix [26]. Results showed that the addition of SiC nanoparticles was able to enhance tensile strength and ductility indicating that a thermally stable bond exists between the reinforcement nanoparticles and the matrix, below recrystallization temperature. The enhanced ductility of the present SiCp/AZ91 nanocomposite could be attributed to the grain refinement after hot extrusion (Fig. 1) as well as the uniform dispersion (Figs. 4 and 5) of thermally stable nanoparticles throughout the matrix. The grains of matrix in the SiCp/AZ91 nanocomposite are significantly refined after hot extrusion. This would obviously result in the improvement of ductility. In addition, based in our present work [17,20], the interface behavior showing no intermediate phases at the interface between SiC nanoparticle and matrix, and found that the SiC nanoparticles were well bonded to the matrix. And no reflection ring of interfacial reaction is found except for reflection ring of Mg and SiC from the study of ED as shown in Fig. 5(d). This can also indicate that the SiC nanoparticles bond well with the matrix in the nanocomposite. Then, SiC nanoparticles aid in maintaining the grain structure in the extruded SiCp/AZ91 nanocomposite by pinning grain boundaries at elevated temperatures thus resulting in higher ductility.

4. Conclusions

The SiCp/AZ91 magnesium matrix nanocomposite fabricated by semisolid stirring assisted ultrasonic vibration is extruded at 350 °C with an extrusion ratio of 12:1. The main results of the work can be summarized as follows:

(1) Large scale dynamic recrystallization is observed in the extruded SiCp/AZ91 nanocomposite with an average grain size of ~6 μm. The grains of the SiC nanoparticle bands are finer than that in the refined grain zones.
(2) Distribution of SiC nanoparticles in the SiCp/AZ91 nanocomposite is improved due to the extrusion process. Although some agglomerates of SiC nanoparticles still exist in the SiC nanoparticle bands, the distribution of SiC nanoparticle is homogeneous outside the SiC nanoparticle bands.
(3) It is shown that after extrusion the SiCp/AZ91 nanocomposite exhibits a simultaneous increase in yield strength, ultimate tensile strength and elongation to fracture. Compared with the extruded AZ91 alloy the yield strength and ultimate tensile strength of the extruded SiCp/AZ91 nanocomposite are enhanced while elongation to fracture is slightly decreased.
(4) Tensile strength of SiCp/AZ91 nanocomposite is enhanced compared with the AZ91 alloy under all the test temperatures while the ductility is improved with the temperature range from 75 to 225 °C.

Acknowledgment

This work was supported by “National Natural Science Foundation of China” (No. 51101043) and “the Fundamental Research Funds for the Central Universities” (Grant No. HIT.NSRIF.201130).

References

[1] S.Y. Liu, F.P. Gao, Q.Y. Zhang, X. Zhu, W.Z. Li, Trans. Nonferrous Met. Soc. China 20 (2010) 1222–1227.
[2] Q.C. Jiang, H.Y. Wang, B.X. Ma, Y. Wang, F. Zhao, J. Alloys Compd. 386 (2005) 177–181.
[3] X.J. Wang, K. Wu, W.X. Huang, H.F. Zhang, M.Y. Zheng, D.L. Peng, Compos. Sci. Technol. 67 (2007) 2253–2260.
[4] H.Z. Ye, X.Y. Liu, J. Alloys Compd. 402 (2005) 162–169.
[5] Y. Wang, H.Y. Wang, Y.F. Yang, Q.C. Jiang, Mater. Sci. Eng. A 478 (2008) 9–15.
[6] P. Poddar, V.C. Srivastava, P.K. De, K.L. Sahoo, Mater. Sci. Eng. A 518 (2007) 357–364.
[7] S.H. Chen, P.P. Jin, G. Schumacher, N. Wanderka, Compos. Sci. Technol. 70 (2010) 123–129.
[8] S.J. Wang, G.Q. Wu, Z.H. Ling, Z. Huang, Mater. Sci. Eng. A 518 (2009) 158–161.
[9] V. Viswanathan, T. Laha, K. Balani, A. Agarwal, S. Seal, Mater. Sci. Eng. R 54 (2006) 121–285.
[10] M. Habibnejad-Korayem, R. Mahmudi, W.J. Poole, Mater. Sci. Eng. A 519 (2009) 198–203.
[11] Q.B. Nguyen, M. Gupta, J. Alloys Compd. 490 (2010) 382–387.
[12] S.F. Hassan, M. Gupta, J. Alloys Compd. 429 (2007) 176–183.
[13] S.F. Hassan, T. Khin Sandar, M. Gupta, J. Alloys Compd. 509 (2011) 4341–4347.
[14] W.L.E. Wong, M. Gupta, Compos. Sci. Technol. 67 (2007) 1541–1552.
[15] C.J. Lee, J.C. Huang, P.J. Hsieh, Scripta Mater. 54 (2006) 1415–1420.
[16] L. Lü, M.O. Lai, W. Liang, Compos. Sci. Technol. 64 (2004) 2009–2014.
[17] K.B. Nie, X.J. Wang, X.S. Hu, L. Xu, K. Wu, M.Y. Zheng, Mater. Sci. Eng. A 528 (2011) 5278–5282.
[18] J. Lan, Y. Yang, X. Li, Mater. Sci. Eng. A 386 (2004) 284–290.
[19] G. Cao, H. Konishi, X. Li, Mater. Sci. Eng. A 486 (2009) 357–362.
[20] K.B. Nie, X.J. Wang, K. Wu, L. Xu, M.Y. Zheng, X.S. Hu, J. Alloys Compd. 509 (2011) 8664–8669.
[21] K.S. Suslick, Annu. Rev. Mater. Sci. 29 (1999) 295–326.
[22] M.J. Tan, X. Zhang, Mater. Sci. Eng. A 244 (1998) 80–85.
[23] T.V. Clyne, P.J. Withers, An Introduction to Metal Matrix Composites, Cambridge University Press, Cambridge, 1993.
[24] K.K. Deng, K. Wu, X.J. Wang, Y.W. Wu, X.S. Hu, M.Y. Zheng, W.M. Gan, H.G. Brokmeier, Mater. Sci. Eng. A 527 (2010) 1630–1635.
[25] V.V. Bhanu Prasad, B.V.R. Bhat, Y.R. Mahajan, P. Ramakrishnan, Mater. Manuf. Process. 16 (2001) 841–853.
[26] H. Choi, N. Alba-Baena, S. Nimityongskul, M. Jones, T. Wood, M. Sahoo, R. Lakes, S. Kou, X. Li, J. Mater. Sci. 46 (2011) 2991–2997.
[27] X.J. Wang, K. Wu, H.F. Zhang, W.X. Huang, H. Chang, W.M. Gan, M.Y. Zheng, D.L. Peng, Mater. Sci. Eng. A 465 (2007) 78–84.
[28] H.Z. Ye, X.Y. Liu, J. Mater. Sci. 39 (2004) 6153–6171.